# Dispersion relations, capillary waves, and the Rayleigh-Plateau instability

Claudiu PATRASCU*,[1], Corneliu BALAN[1]

*Corresponding author
[1]"POLITEHNICA" University of Bucharest,
Splaiul Independenţei 313, 060042, Bucharest, Romania,
claudiu.patrascu@upb.ro*, corneliu.balan@upb.ro

DOI: 10.13111/2066-8201.2022.14.2.7

*Received: 10 November 2021/ Accepted: 22 March 2022/ Published: June 2022*


***Abstract:*** *The paper shows the importance of the dispersion relation in characterizing the capillary waves seen on liquid jets. Several theoretical models are given to better understand the stability of cylindrical interfaces when various parameters are considered, such as confinement, bulk elasticity, or the viscosity ratio between the two liquid phases. Theoretical predictions are compared with experimental data in terms of the fastest-growing mode for several liquid-in-air systems. Capillary-wave decay factors are also investigated, for stationary wave trains created at the impact of a liquid jet on a horizontal liquid bath, via the dispersion relation.*

***Key Words:*** *capillary waves; Rayleigh instability; dispersion relation; growth rate*

## 1. INTRODUCTION

When a liquid is injected through a capillary tube at a constant flow rate, which ensures the formation of a liquid jet, the free surface naturally develops waves.

This is an example of hydrodynamic instability which is known as Rayleigh-Plateau instability triggered by capillary forces acting at the free surface of the jet.

The ultimate effect of the perturbations, which dominate free surfaces, is the formation of droplets. Perturbations grow until their amplitude reaches the value of the unperturbed thread's radius, at which point a droplet is created.

In this way, the system naturally evolves towards a state which lowers the surface energy. The process is periodic, making jets a reliable and predictable "machine" at creating drops.

The growth rate will affect the length of the jet, whilst the dominant wavelength will give the diameter of the droplet.

Any perturbation can grow, decay, or persist with the same magnitude, describing unstable, stable, or neutrally stable regimes.

Figure 1 shows a series of unstable interfaces where perturbations grow in a wave-like manner. This type of instability is known as Rayleigh-Plateau instability.

The perturbation grows in time and, due to its oscillatory nature, it induces a local decrease in diameter which increases the capillary pressure. When the perturbation amplitude reaches the unperturbed thread's radius, breakup occurs.

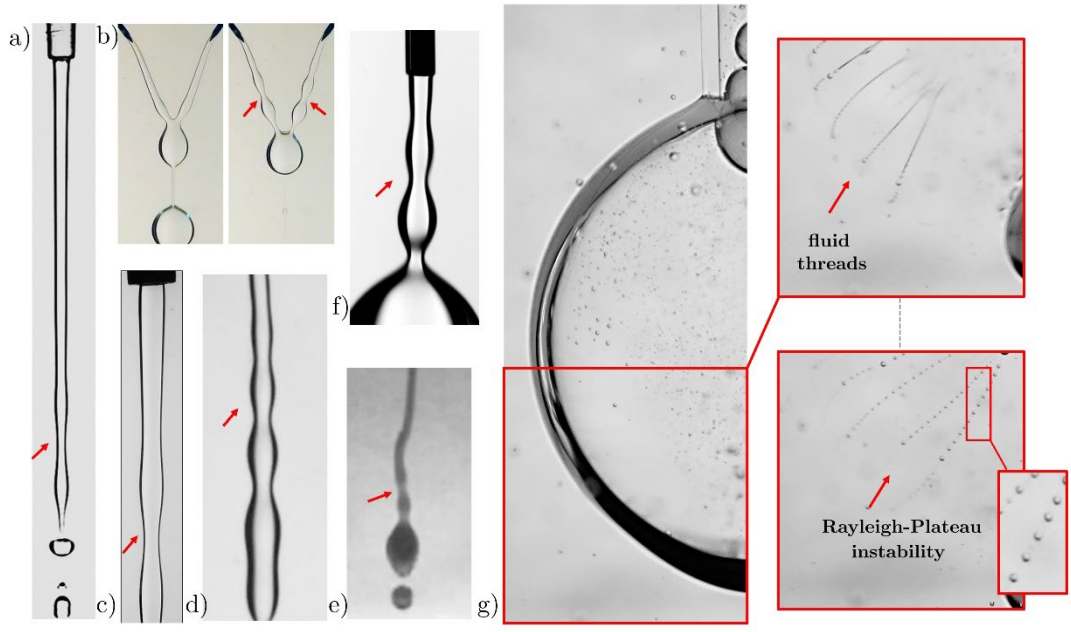


Fig. 1 Series of unstable interfaces as Rayleigh-Plateau instability develops: a) water jet in air; b) coalescent liquid volumes; c) immersed viscoelastic jets ; d), e), f) immersed water jets in sunflower-seed oil; g) burst of a water "double", a thin water interface surrounded on each side by a viscous oil (the name is extrapolated from soap bubble, which is a thin liquid interface having air on both sides)

The breakup length represents the distance from the capillary to the point of breakup. One can show that the breakup length $L_b$ can be estimated by knowing the growth rate $\omega$ of the dominant mode ($L_b \propto V/\omega$, where $V$ is the average flow velocity) and that the diameter of the main drop $D_d$ is directly related to the wavenumber $k$ of the perturbation ($D_d^3 \propto R_0^2/k$, where $R_0$ is the unperturbed jet radius). Due to the nonlinearity of the final stages of breakup, often one also observes satellite droplets, much smaller in diameter than the main drop.

Dispersion relations (growth rate $\omega$ as a function of the wavenumber$k$) describe the instability of liquid threads under the action of the surface tension. A series of examples of unstable interfaces is given in figure 1. The first who derived a dispersion relation for a cylindrical liquid jet was Rayleigh [1]. For the case of an infinitely long cylindrical thread in a quiescent external gas, the dispersion relation is given by

$$\omega^2 = \frac{\sigma}{\rho R_0^3} kR_0(1 - k^2R_0^2)\, I_1(kR_0)/I_0(kR_0), \tag{1}$$

where $I_{1,2}$ are the modified Bessel functions of the first kind, $k$ is the wavenumber, $R_0$ is the unperturbed jet's radius, $\rho$ is the fluids density, and $\sigma$ the superficial tension.

Rayleigh extends the stability analysis for viscosity dominated flows and gives an approximation of the dispersion relation as [2]

$$\omega = \frac{\sigma}{6\eta R_0}(1 - k^2R_0^2), \tag{2}$$

where $\eta$ is the viscosity of the liquid.

The predictions of equations (1) and (2) can be combined in a single dispersion relation [3] given by

$$\omega^2 = \frac{\sigma}{\rho R_0^3}\left[\left(\frac{1}{2}k^2\,R_0^2(1-k^2R_0^2)+\frac{9}{4}Oh^2k^4\,R_0^4\right)^{0.5}-\frac{3}{2}Oh\,k^2\,R_0^2\right]^2. \quad (3)$$

The above equation yields an exact expression for the critical wavenumber, given by

$$\frac{1}{kR_0} = \sqrt{2+3\sqrt{2}Oh} \quad (4)$$

where $Oh$ is the Ohnesorge number $\left(Oh = \eta/\sqrt{\rho\sigma R_0}\right)$.

In the case of a hollow jet one finds [3]

$$\omega^2 = \frac{\sigma}{\rho R_0^3}kR_0(1-k^2R_0^2)\,K_1(kR_0)/\,K_0(kR_0), \quad (5)$$

Usually, the effect of gravity is neglected since the phenomena is dominated by capillarity (i.e. Bond numbers lower than unity).

At large length scales, the gravitational induced collapse of a cylindrical fluid structure is given by [4]

$$\omega^2 = 4\pi G\rho kR_0\,\frac{I_1(kR_0)}{I_0(kR_0)}\left[\frac{1}{2}-K_0(kR_0)I_0(kR_0)\right], \quad (6)$$

where $G$ is the gravitational constant.

For a viscous thread surrounded by another viscous immiscible liquid, Tomotika [5] showed, in the limit of Stokes flow, that

$$\omega = \frac{\sigma}{2\eta_e R_0}(k^2R_0^2-1)f(kR_0,\beta), \quad (7)$$

a dispersion relation which is also dependent on the viscosity ratio $\beta = \eta_i/\eta_e$, where $\eta_i$ is the viscosity of the inner phase and $\eta_e$ the viscosity of the external one. Further details about dispersion relations and their derivation can be found in [6].

Positive values for the growth rate imply instability, whereas negative values imply stable fluid threads (see figure 2-b). Figure 2-c shows the dispersion relations for an inviscid, a highly viscous, and a hollow jet.

## 2. CHARACTERISTIC PARAMETERS

The instability can manifest spatially, where perturbations can move in the opposite direction of the flow and cause a dripping regime near the capillary tip.

Figure 3 depicts the dripping to jetting transition and the atomization of a liquid water jet submerged in viscous oil.

As the flow rate is increased, convective forces will overcome the surface tension and a jetting regime will settle.

In this regime, the breakup length increases linearly with the average flow velocity. By increasing the flow rate even further, the viscous stresses become important, the breakup length decreases, and the atomization of the jet occurs.

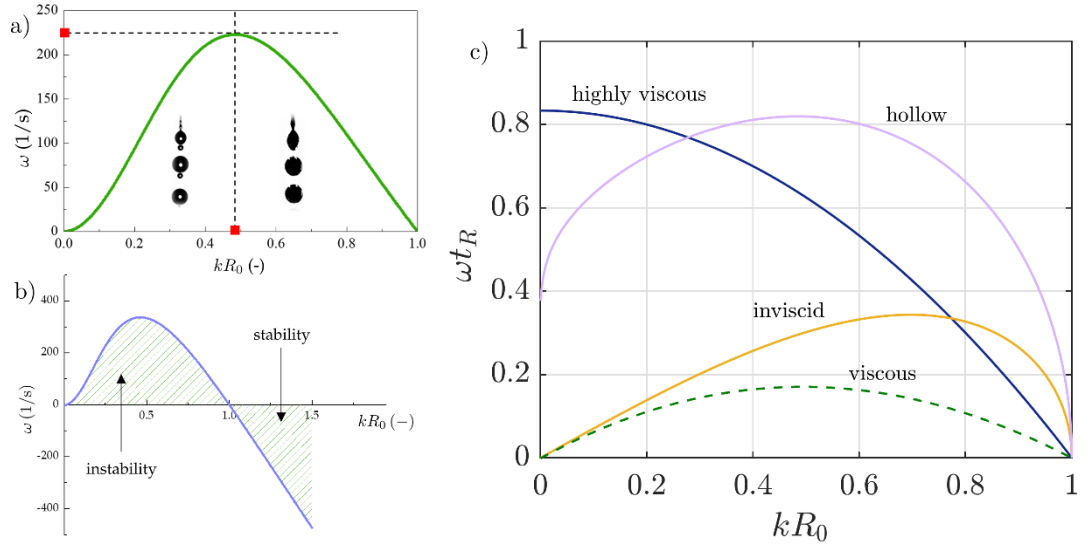


Fig. 2 a) Growth rate $\omega$ as a function of the dimensionless wavenumber $kR_o$. In some cases, the occurrence of satellite droplets can be avoided if one drives the jet at a wavenumber above the critical threshold. Only positive values imply instability (b), the dominant wave being set by the dispersion curve's maximum. c) Dispersion curves for: an inviscid jet given by eqn. (1), a viscous jet when $Oh = 0.5$ given by eqn. (3), a hollow jet given by eqn. (5) and a highly viscous jet, $Oh = 5$, given by eqn. (2). Here, $t_R = (\rho R_0^3 / \sigma)^{0.5}$ is the Rayleigh time scale.

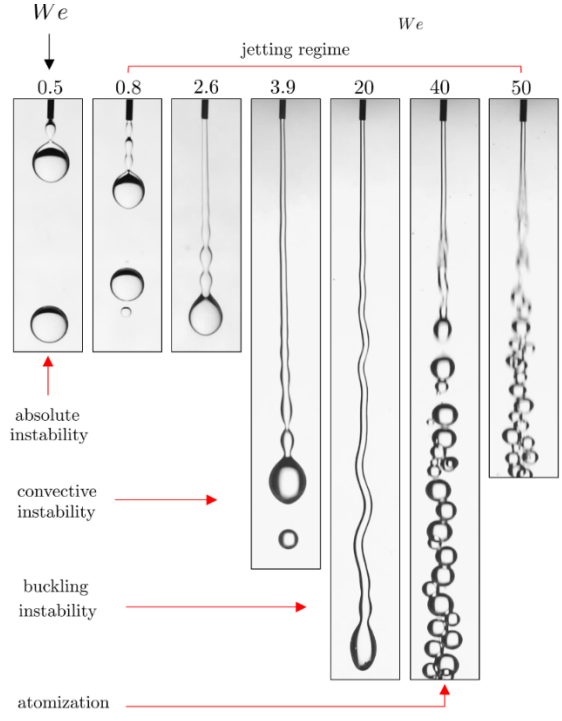


Fig. 3 Different types of unstable jets as the Weber number increases; from dripping, to jetting, to buckling and atomization

The nondimensional parameter which describes the limit between dripping and jetting is the Weber number,

$$We = \frac{\rho V^2 R_0}{\sigma}, \tag{8}$$

the ratio between the convective forces and the surface tension forces, or the ratio between the average flow velocity and the capillary velocity $V_c = [\sigma/(\rho R_0)]^{0.5}$, $We = (V/V_c)^2$.

If $We \gg 1$ one usually observes a jet-like structure of the ejected liquid. The ratio of viscous stresses to capillary pressure yields the capillary number,

$$Ca = \frac{\eta V}{\sigma}, \tag{9}$$

an important parameter when viscous forces dominate inertia.

One can combine $We$ and $Ca$ numbers in a single, kinematic-free, parameter which is known as the Ohnesorge number,

$$Oh = \frac{Ca}{\sqrt{We}} = \frac{\eta}{\sqrt{\rho\sigma R_0}}. \tag{10}$$

This parameter can also be defined as the ratio between the inertio-capillary time (i.e., Rayleigh time) and the viscous time scale, namely $Oh = t_v/t_R$, where $t_R = (\rho R_0^3/\sigma)^{0.5}$ and $t_v = \eta R_0/\sigma$.

Capillary forces dominate the dynamics of fluid systems when their proper length scale is below the capillary length,

$$l_c = \sqrt{\frac{\sigma}{\Delta\rho g}}, \tag{11}$$

where $\sigma$ is surface/interfacial tension, $\Delta\rho$ the density difference, and $g$ the acceleration due to gravity.

Figure 4 shows the capillary length of commonly used liquids as a function of their surface tension. The graph shows an "upper bound" of 2.7 mm set by water, therefore the fluid systems below this threshold value will be dominated by the surface forces. The range/ domain of surface forces can be extended by adding an immiscible external liquid. Since the threshold value (i.e. the capillary length) is inversely proportional with the density difference, the addition of the external liquid contributes to the above-mentioned expansion.

Newtonian free surface flows of one liquid can be described in a dimensionless 2D map having the Weber and the capillary numbers as main parameters [9]. If one considers a second immiscible liquid phase, the number of parameters doubles. As an example, one could take the breakup length of a liquid jet surrounded by another immiscible liquid. One can show the following functional relation exists for the breakup length:

$$L_b = f(\rho_i, \rho_e, \eta_i, \eta_e, \sigma, V, R_0), \tag{12}$$

where, the lower indices *i* or *e* denote the dispersed (injected) or the continuous (external) phase, respectively.

All quantities can be reduced to three fundamental units (mass, length, and time), and by virtue of dimensional analysis the functional relation can be rewritten as a combination of five dimensionless parameters, namely:

$$\frac{L_b}{R_0} = f(We_i, Ca_i, \zeta, \beta). \tag{13}$$

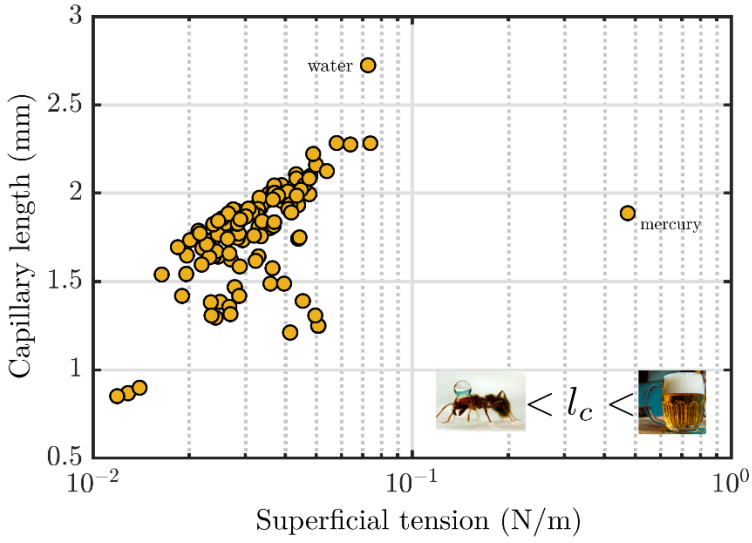


Fig. 4 Capillary length, given by eqn. (11), as a function of surface tension for a series of common liquids. Material and surface properties partially taken from [7,8]

It is observed that in the presence of an exterior liquid phase the number of relevant dimensionless parameters doubles. The abstract 4D map will now include the density ratio, $\zeta = \rho_i/\rho_e$, and the viscosity ratio, $\beta = \eta_i/\eta_e$. Mapping the entire parameter 4D space is a difficult task due to the wide range of the viscosity contrast seen in Newtonian systems. If non-Newtonian fluids are also taken into account the problem becomes almost impossible to tackle in a single general framework.

## 3. EXTENDED STUDIES OF THE RAYLEIGH-PLATEAU INSTABILITY

Besides the viscosity of the injected fluid, the capillary instability of a cylindrical liquid thread can be affected by several other factors, such as the presence of surfactant at the separating interface, crossflow, viscoelasticity, confinement, a viscous or viscoelastic immiscible outer liquid, curvature elasticity, nozzle geometry, slip at the interface or the presence of an electrical field [10].

The dispersion relation derived by Tomotika for the case of a cylindrical liquid thread surrounded by another immiscible liquid is given by the following equation:

$$\omega = \frac{\sigma}{2\eta_e R_0}(k^2 R_0^2 - 1) f(kR_0, \beta), \tag{14}$$

where $\beta$ is the viscosity ratio between the inner and the outer liquid phase.

The exact for of $f(kR_0, \beta)$ can be found in Tomotika's original paper [5]. In comparison with the classical case of a liquid jet in air, it shows the stabilizing effect of an external liquid on Rayleigh-Plateau instability.

Also, the increase of the viscosity ratio will always bring with it lower values for the growth rate of instability.

The most unstable wavenumber, however, increases with the viscosity ratio when $\beta < 0.3$ and decreases otherwise. This implies that longer wavelengths dominate the thread when $\beta > 0.3$.

This threshold can be changed if one considers a solid cylindrical wall that confines the external liquid.

The dispersion relation will now be dependent also on the confinement ratio $\alpha = R_c/R_0$, where $R_c$ is the radius of the cylindrical wall,

$$\omega = \frac{\sigma}{2\eta_e R_0}(k^2 R_0^2 - 1) f(\alpha, \beta, kR_0). \tag{15}$$

The dispersion relation shows the stabilizing effect of confinement for any viscosity ratio [11]. Also, a change is observed in the value of the critical viscosity ratio for which longer wavelengths dominate the liquid thread.

For smaller values of the confinement ratio (the wall is closer to the thread) the critical viscosity ratio increases (see figure 5-a).

Viscoelasticity is known for the destabilizing effect it produces. If one considers a viscoelastic thread surrounded by another immiscible Newtonian liquid, the dispersion relation will become dependent on the elasto-capillary number, $Ec = \mu_i \sigma/\eta_{i,0} R_0$, where $\mu_i$ is the relaxation time of the material,

$$\omega = \frac{\sigma}{2\eta_e R_0}(k^2 R_0^2 - 1) f(\beta, kR_0, Ec). \tag{16}$$

As depicted by figure 5-b, the presence of viscoelasticity in the injected liquid increases the growth rate, thus leading to less stable cylindrical columns [12, 13].

The dispersion relation can also be of help when studying impinging liquid jets. The capillary waves are seen at the base of the quasi-cylindrical column decay in the opposite direction of the flow, their wavelength and decay factor being given the dispersion relation [14]. Figure 6 shows capillary waves at the base of a liquid jet and the measured amplitude at each wave crest.

The suppression of the capillary-wave field has been shown to occur when increasing the viscosity of the injected liquid by a small amount [15]. The destabilizing effect is shown by considering viscoelasticity via the dispersion relation:

$$[Oh(KR_0 + m)]^2 + KR_0\left[f^2 - 4Oh^2\sqrt{m\,KR_0}\right] = 0, \tag{17}$$

where $m$ is a function of Reynolds and Deborah numbers and $K$ is the complex wavenumber having the real part as the wavenumber and the imaginary part as the decay factor [15].

Other dispersion relations can also be found in [16-20].

## 4. CAPILLARY RAYLEIGH MODES ON FREE LIQUID JET

When a liquid is being pumped through a capillary tube, in air, at a constant flow rate, when $We \gg 1$ a liquid jet will form and break into droplets at a certain distance downstream.

The free surface will naturally develop a perturbation with a wavelength given by the fastest-growing mode.

To show this, one seeks to compare the predictions in terms of the wavelength of the fastest-growing mode with the experimental data. The wavelength can be approximated by the following equation [3].

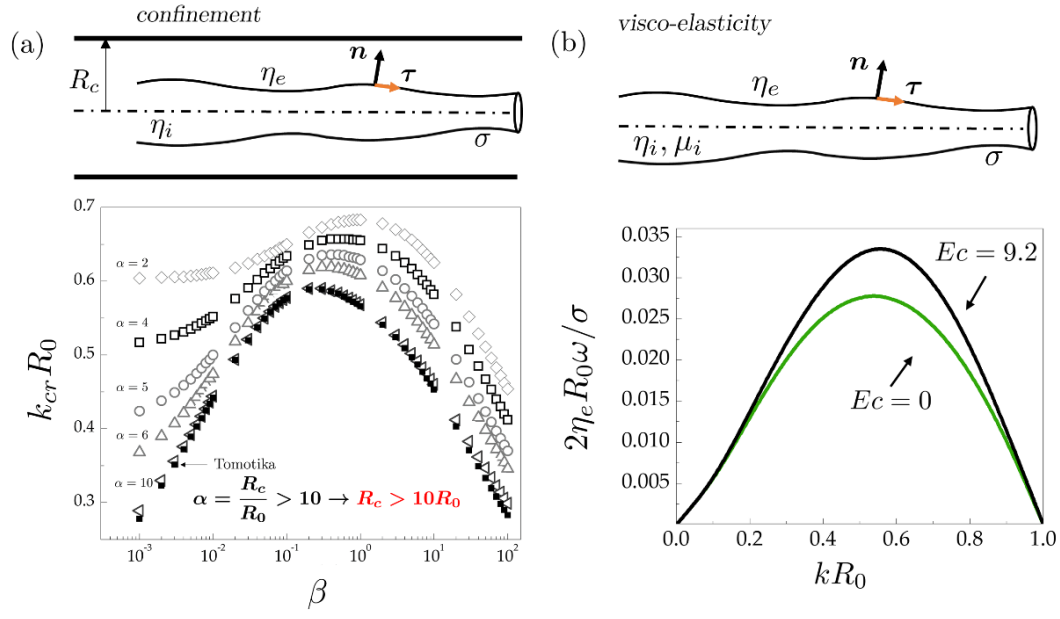


Fig. 5 a) The effect of the confinement ratio $\alpha$ on the most unstable wavenumber $k_{cr}R_0$ as a function of the viscosity ratio $\beta$. b) Comparison between the dispersion curve for a two-liquid system and the dispersion relation (in dimensionless form) in the case of a viscoelastic inner liquid when $Ec = 9.2$.

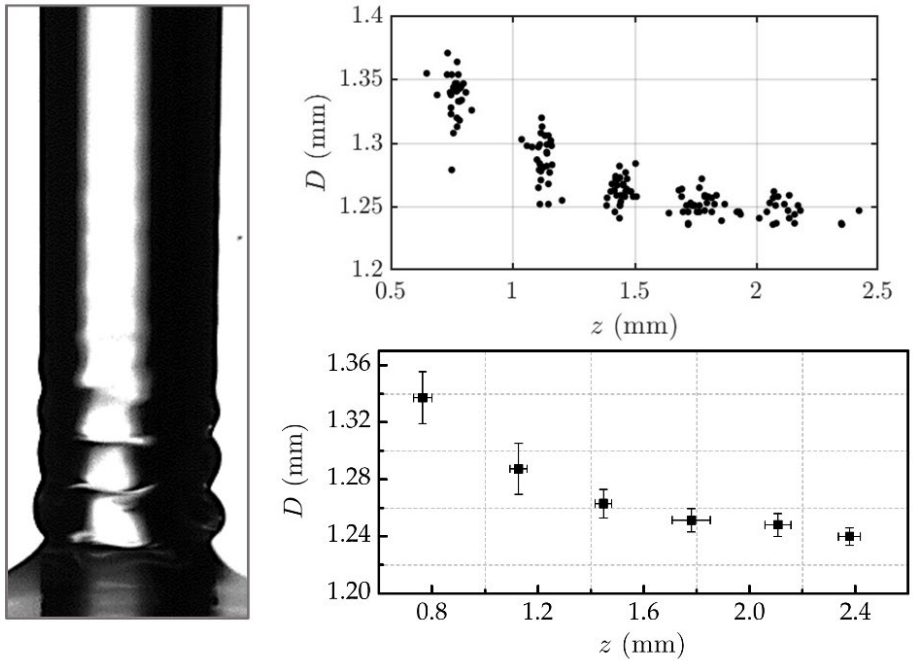


Fig. 6 Capillary waves at the base of an impinging liquid jet (right) and the measured wave-crest amplitude for a water jet of 1.2 mm in diameter. Error bars are shown for each set of data points

$$\frac{\lambda}{\pi D_0} = \sqrt{2 + 3\sqrt{2}Oh}\,, \tag{18}$$

where $Oh = \eta/(\rho R_0 \sigma)^{0.5}$ is the Ohnesorge number.

For an inviscid fluid, $Oh \to 0$, the predictions agree with the most unstable wavenumber predicted by Rayleigh's theory, $\lambda = \sqrt{2}\,\pi\, D_0$, i.e., $kR_0 \approx 0.7$ (see figure 7-b). The equation also shows larger wavelengths when the Ohnesorge number increases.

Five different test liquids are injected through a 1.8 mm diameter capillary tube. The material properties of the working fluids are given in table 1.

The jet will decrease in radius because of the gravitational field until the thread starts to show capillary instability.

Together with the measurements of the wavelength, one must measure the thread's initial diameter $D_0$, which was taken as the jet diameter upstream the perturbation where no fluctuation was observed.

A series of jets and their dominant mode is shown in figure 7-a. The main findings can be summarized as follows: *i*) the experimental data agree well with the predicted values, $kR_0 \approx 0.7$, in the case of a water jet at different flow rates (see figure 8-a); *ii*) the jet formation when $We > 4$ which agrees with the theoretical predictions for low Ohnesorge and Bond numbers; *iii*) the dominant wavelength exceeds the circumference of the thread, excellent agreement being observed when $We > 10$ in the case of water jets (see figure 8-b); *iv*) there is a good qualitative agreement with eqn. (18) for all test fluids.

The dominant wavelength increases with the Ohnesorge number, being always greater than the circumference of the unperturbed state

Table 1. Material properties of the working liquids

| Fluid | $D_0$ $(mm)$ | $\eta$ $(mPa\,s)$ | $\sigma$ $(N/m)$ | $\rho$ $(kg/m^3)$ |
|---|---|---|---|---|
| Water | 1.47 | 1 | 0.075 | 998 |
| Water+glycerine | 1.33 | 2 | 0.072 | 1056 |
| Water+glycerine | 1.38 | 10 | 0.070 | 1150 |
| Mercury | 1.46 | 1.5 | 0.450 | 13590 |
| Sunflower-seed oil | 1.48 | 55 | 0.030 | 920 |

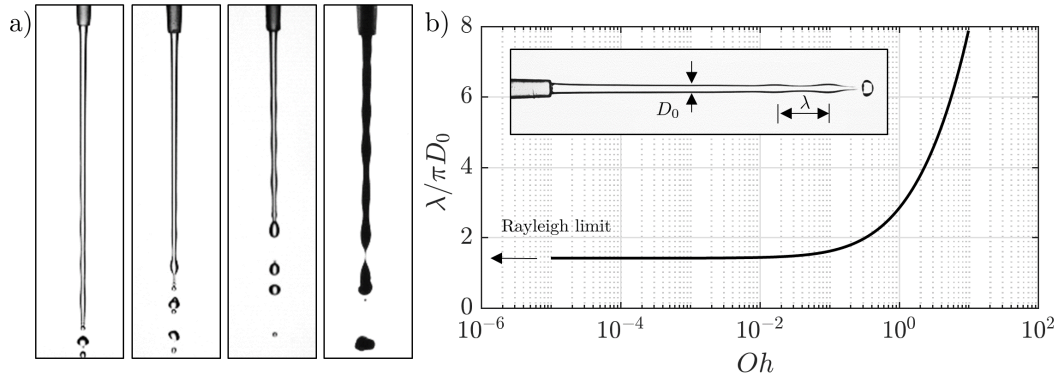


Fig. 7 a) Series of jets and depiction of their dominant mode. From left to right the fluids are those given in table 1. b) Dimensionless wavelength as a function of the Ohnesorge number as predicted by equation (18). When $Oh \to 0$, one recovers Rayleigh's result for an inviscid fluid [1].

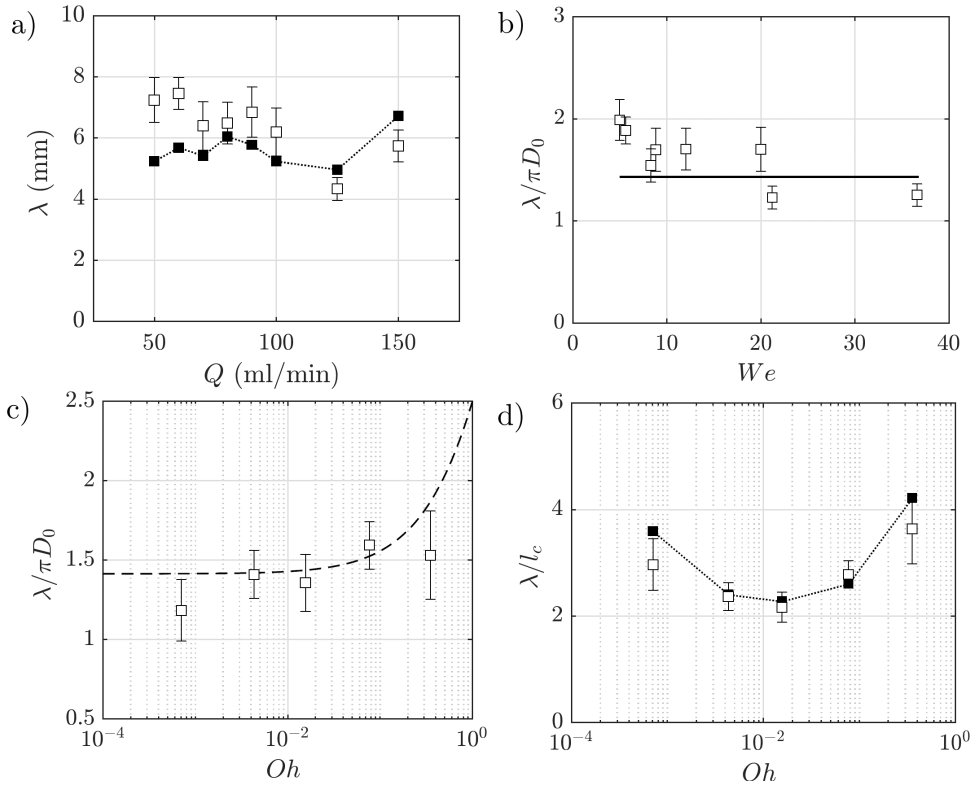


Fig. 8 a) Experimental data vs. theoretical values for water jets at different flow rates. b) Dimensionless wavelength for different values of the Weber number. The continuous line represents Rayleigh's prediction for an inviscid fluid, $\lambda = \sqrt{2}\pi D_0$. c) Dimensionless wavelength as a function of the Ohnesorge number (the broken line is given by equation (18). d) Number of capillary lengths shown by the wavelength of the dominant mode for several values of the Ohnesorge number. The filled symbols are given by theory. $Q \approx$ 50 ml/min when not specified.

(see figure 8-c). The number of capillary lengths of each dominant wavelength, $\lambda/l_c$, is always greater than two (see figure 8-d).

The more viscous jet tends to dampen perturbations and thin to relatively small dimensions where non-linearity prevails.

This is probably the main cause of the large dispersion of data shown in figure 8-c for $Oh = 0.3554$.

## 5. CONCLUSIONS

The paper emphasizes the stabilizing effect of viscosity, confinement, and a viscous immiscible outer liquid phase on the capillary instability of a cylindrical liquid thread via the dispersion relation. Stationary capillary waves can also be described in terms of wavelength and decay factor by analyzing the correspondent dispersion curve. A viscosity stabilizing effect and a viscoelasticity destabilizing effect are observed. The emergence of a dominant mode is qualitatively shown, through a series of experiments, as a function of the Ohnesorge number.

## ACKNOWLEDGEMENT

The paper represents an extended abstract of the doctoral thesis of the first author, Claudiu Patrascu, for which he received the "Nicolae Tipei" Prize in 2021 at the *39th "Caius Iacob" Conference on Fluid Mechanics and its Technical Applications, 28 – 29 October 2021, Bucharest, Romania (Virtual Conference)*, from Prof. dr. Sever Tipei, University Illinois, USA, in partnership with INCAS – National Institute for Aerospace Research "Elie Carafoli". The experimental investigations were possible due to European Regional Development Fund through Competitiveness Operational Program 2014-2020, Priority axis 1, Project No. P_36_611, MySMIS code 107066, Innovative Technologies for Materials Quality Assurance in Health, Energy and Environmental - Center for Innovative Manufacturing Solutions of Smart Biomaterials and Biomedical Surfaces – INOVABIOMED. The authors acknowledge the support of CHIST-ERA – 19 – XAI – 009 MUCCA project, by the founding of EC and The Romania Executive Agency for Higher Education, Research, Development and Innovation Funding - UEFISCDI, grant COFUND-CHIST-ERA MUCCA no. 206/2019.

## REFERENCES

[1] L. Rayleigh, On the instability of jets, *Proceedings of the London Mathematical Society*, **1**(1), 4-13, 1878.
[2] L. Rayleigh, XVI. On the instability of a cylinder of viscous liquid under capillary force, *The London, Edinburgh, and Dublin Philosophical Magazine and Journal of Science*, **34**(207), 145-154, 1892.
[3] J. Eggers & E. Villermaux, Physics of liquid jets, *Reports on Progress in Physics*, **71**(3), 036601, 2008.
[4] S. Chandrasekhar, *Hydrodynamic and hydromagnetic stability*, Courier Corporation, 2013.
[5] S. Tomotika, On the instability of a cylindrical thread of a viscous liquid surrounded by another viscous fluid, *Proceedings of the Royal Society of London. Series A-Mathematical and Physical Sciences*, **150**(870), 322-337, 1935.
[6] B. J. Meister & G. F. Scheele, Generalized solution of the Tomotika stability analysis for a cylindrical jet, *AIChE Journal*, **13**(4), 682-688, 1967.
[7] D. R. Lide & G. W. Milne, *Handbook of data on common organic compounds*, CRC press, 1995.
[8] * * * *Surface tension of organic fluids*, http://www.surface-tension.de/, Accesed: 08-22-2020.
[9] C. Clasen, P. M. Phillips, L. Palangetic & A. J. Vermant, Dispensing of rheologically complex fluids: The map of misery, *AIChE Journal*, **58**(10), 3242-3255, 2012.
[10] J. M. Montanero & A. M. Ganán-Calvo, Dripping, jetting and tip streaming, *Reports on Progress in Physics*, **83**(9), 097001, 2020.
[11] C. Patrascu & C. Balan, The stabilizing effect of confinement on a liquid jet in a viscous outer fluid, *UPB Sci. Bull., Series A*, **81**(3), 85-94, 2019.
[12] G. Brenn, Z. Liu & F. Durst, Linear analysis of the temporal instability of axisymmetrical non-Newtonian liquid jets, *International Journal of Multiphase Flow*, **26**(10), 1621-1644, 2000.
[13] C. Patrascu & C. Balan, Prediction and measurement of the fastest-growing mode in two-liquid systems, *Physics of Fluids*, **31**(8), 083106, 2019.
[14] K. M. Awati & T. Howes, Stationary waves on cylindrical fluid jets, *American Journal of Physics*, **64**(6), 808-811, 1996.
[15] C. Patrascu & C. Balan, Decay of stationary capillary waves on impinging liquid jets, *Physics of Fluids*, **33**(2), 022109, 2021.
[16] C. Patrascu & C. Balan, The effect of curvature elasticity on Rayleigh–Plateau instability, *European Journal of Mechanics-B/Fluids*, **80**, 167-173, 2020.
[17] F. Gallaire & P. T. Brun, Fluid dynamic instabilities: theory and application to pattern forming in complex media, *Philosophical Transactions of the Royal Society A: Mathematical, Physical and Engineering Sciences*, **375**(2093), 20160155, 2017.
[18] V. Cardoso & O. J. Dias, Rayleigh-Plateau and Gregory-Laflamme instabilities of black strings, *Physical Review Letters*, **96**(18), 181601, 2006.
[19] C. Zhao, J. E. Sprittles & D. A. Lockerby, Revisiting the Rayleigh – Plateau instability for the nanoscale, *Journal of Fluid Mechanics*, **861**, 2019.
[20] K. Graessel, C. Bächer & S. Gekle, Rayleigh–Plateau instability of anisotropic interfaces. Part 1. An analytical and numerical study of fluid interfaces, *Journal of Fluid Mechanics*, **910**, 2021.